Chemistry – An Asian Journal

CHEMISTRY AN ASIAN JOURNAL | ACES Asian Chemical Editorial Society

RESEARCH ARTICLE OPEN ACCESS

Aggregation-Induced Energy Transfer Within a Donor–Acceptor–Donor Compound Featuring Hydrophobic Mesogenic Self-Assembling Units

Ryota Usami[1] | Koichiro Ishibashi[2] | Nae Aota[1] | Go Watanabe[2,3] | Yoshiya Omori[4] | Tsuneaki Sakurai[4] | Masaki Shimizu[4] | Satoshi Minakata[1] | Youhei Takeda[1]

[1]Department of Applied Chemistry, Graduate School of Engineering, The University of Osaka, SuitaYamadaoka 2-1, 5650871, Japan | [2]Department of Physics, School of Science, Kitasato University, Sagamihara, Kanagawa 2520373, Japan | [3]Department of Data Science, School of Frontier Engineering, Kitasato University, Sagamihara, Kanagawa 2520373, Japan | [4]Faculty of Molecular Chemistry and Engineering, Kyoto Institute of Technology, Hashikami-cho, Matsugasaki, 6068585, Kyoto, Japan

Correspondence: Go Watanabe (go0325@kitasato-u.ac.jp) | Youhei Takeda (takeda@chem.eng.osaka-u.ac.jp)

Received: 21 August 2025 | **Revised:** 27 October 2025 | **Accepted:** 30 October 2025

Keywords: aggregation | charge-transfer | donor-acceptor | energy transfer | luminescence

ABSTRACT

In this study, we report the design and synthesis of a novel donor–acceptor–donor-type organic emitter incorporating hydrophobic starburst mesogenic units. We have demonstrated that, in aqueous environments, this compound undergoes aggregation that induces efficient energy transfer within the molecules, resulting in tunable shifts in emission color. Molecular dynamics simulations corroborate the proposed mechanism by revealing the intramolecular assembly behavior. These findings provide valuable insights for the rational design of functional nano-aggregates targeted for applications in sensing and photonic materials.

1 | Introduction

Organic π-conjugated compounds have attracted considerable attention in materials science due to their unique electro- and photo-active properties arising from extended π-electron systems [1–3]. In particular, their photo-active nature enables diverse applications in optoelectronics [4–6], bioimaging [7], and sensing technologies [8]. Among these, the photophysical properties in the solid state are of increasing relevance, especially for the development of organic light-emitting diodes (OLEDs) [9]. However, conventional organic fluorophores often suffer from aggregation-caused quenching (ACQ) in the condensed phase, primarily due to strong intermolecular electronic interactions and/or exciton delocalization. In this context, the concept of aggregation-induced emission (AIE) [10–12] has opened new avenues for the utilization of organic fluorophores in solid-state environments [5]. A fundamental understanding of how molecular aggregation affects luminescence properties is thus essential for enabling controlled emission behavior via rational molecular assembly design [13].

Previously, we developed dibenzo[*a*,*j*]phenazine (DBPHZ)-cored organic luminophores featuring an electron donor–acceptor–donor (D–A–D) architecture [14], which exhibit a variety of photophysical behaviors, including thermally activated delayed fluorescence (TADF) [15, 16], room-temperature phosphorescence (RTP) [17], and stimuli-responsive luminochromism [18]. Notably, the conformational flexibility of these luminophores plays a crucial role in tuning their emission color. By modulating the population of conformers through external stimuli such as

Dedicated to the memory of Professor Masahiko Iyoda

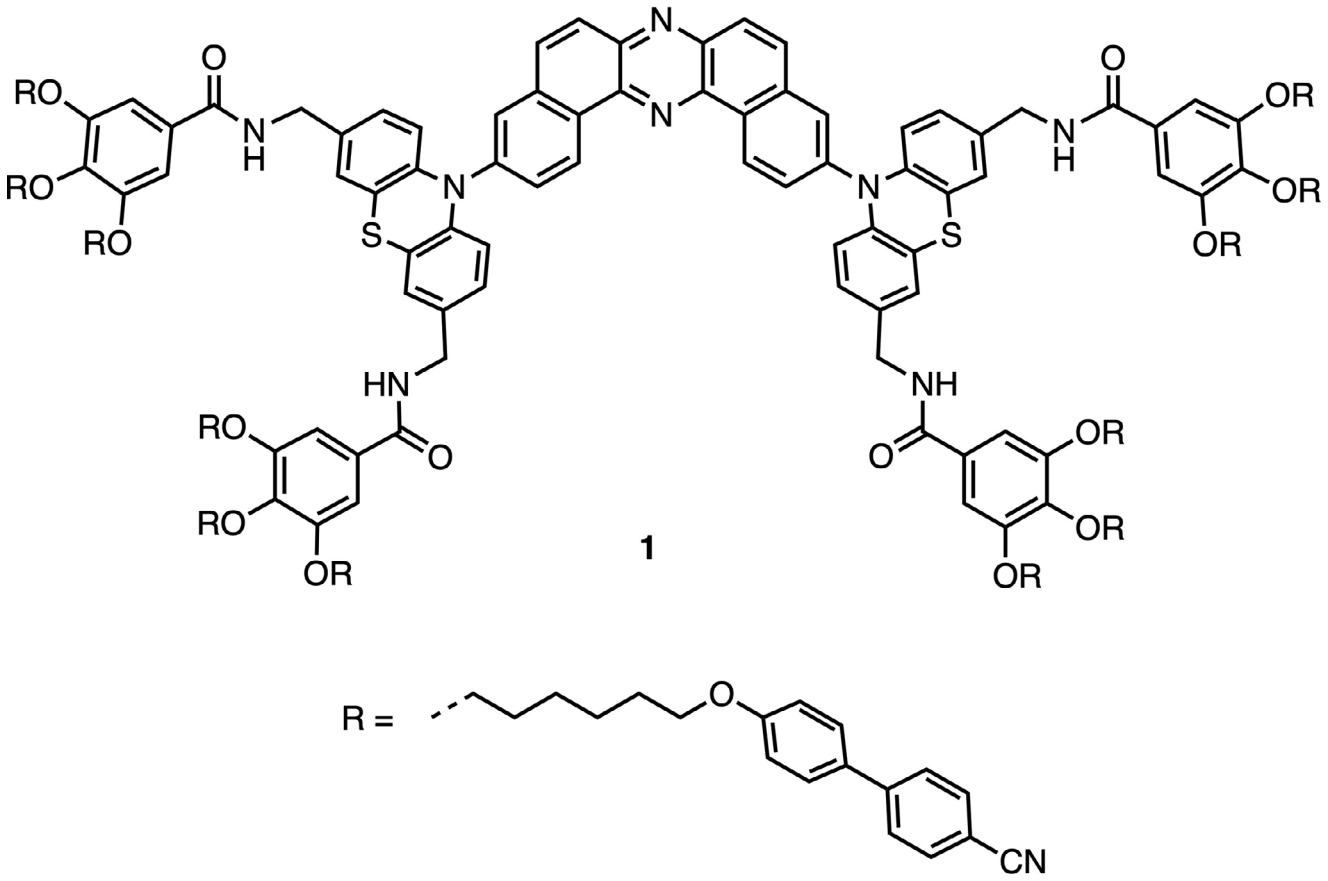

FIGURE 1 | Chemical structure of compound **1**.

anisotropic forces, thermal energy, solvent vapor, or hydrostatic pressure [19], tunable emission characteristics can be achieved. More recently, we introduced six pairs of an amphiphilic self-assembling unit, triethylene glycol monomethyl ether (TEGM), into the D–A–D scaffold containing phenothiazine (PTZ) donor units [20]. This chemical modification facilitated the dispersion of luminophores in aqueous environments and hydrophilic matrices such as polyvinyl alcohol (PVA). Molecular dynamics (MD) simulations revealed the coexistence of conformers originating from different orientations (pseudo-axial or pseudo-equatorial) of the acceptor unit on the boat-chair PTZ donors in aqueous media. Within rigid PVA matrices, these conformers displayed ratiometric emission changes, attributed to their distinct quenching responses toward water molecules. Given the stochastic nature of hydrogen bonding among TEGM units, water, and the PVA matrix, we hypothesized that replacing the hydrophilic self-assembling units with hydrophobic counterparts could provide an effective means to modulate aggregation behavior in aqueous environments. Nevertheless, the influence of such hydrophobic self-assembling units on aggregation and the resulting photophysical properties remains largely unexplored.

Herein, we report the synthesis and aggregation behavior of a novel D–A–D compound, designated as **1**, which incorporates 12 hydrophobic self-assembling units (Figure 1). In aqueous environments, compound **1** exhibits pronounced AIE behavior. Remarkably, its emission properties are tunable depending on the extent of aggregation, a phenomenon attributed to energy transfer (ET) processes within the aggregate. This tunability highlights the potential of compound **1** as a responsive luminescence material application in aqueous environments.

2 | Results and Discussion

2.1 | Design and Synthesis of Materials

As described in the Introduction, we previously developed a water-dispersible D–A–D compound bearing six hydrophilic units on the PTZ donor moieties [20]. To enhance the self-assembling capability in aqueous environments, we conceived the strategy of increasing the number of self-assembling units to elevate the molecular symmetry. As hydrophobic self-assembling units, we took inspiration from the well-known nematic liquid crystal compound 4-cyano-4'-pentylbiphenyl (5CB) and designed a D–A–D compound bearing starburst-type mesogenic groups [21]. Recently, C_3-symmetry multi-resonance TADF molecule incorporating the same mesogenic units has been shown to successfully self-assemble in thin films, enabling controlled molecular orientation for enhanced light out-coupling [22].

The designed compound **1** was synthesized following the synthetic route outlined in Scheme 1 (for detailed experimental procedures, see the Supporting Information). Dibromination of phenothiazine (**2**) using tetra-*n*-butylammonium tribromide [$(n\text{-Bu})_4NBr_3$] as the brominating agent afforded 3,7-dibromophenothiazine (**3**) in high yield. A Pd-catalyzed double Suzuki–Miyaura cross-coupling reaction between dibro-

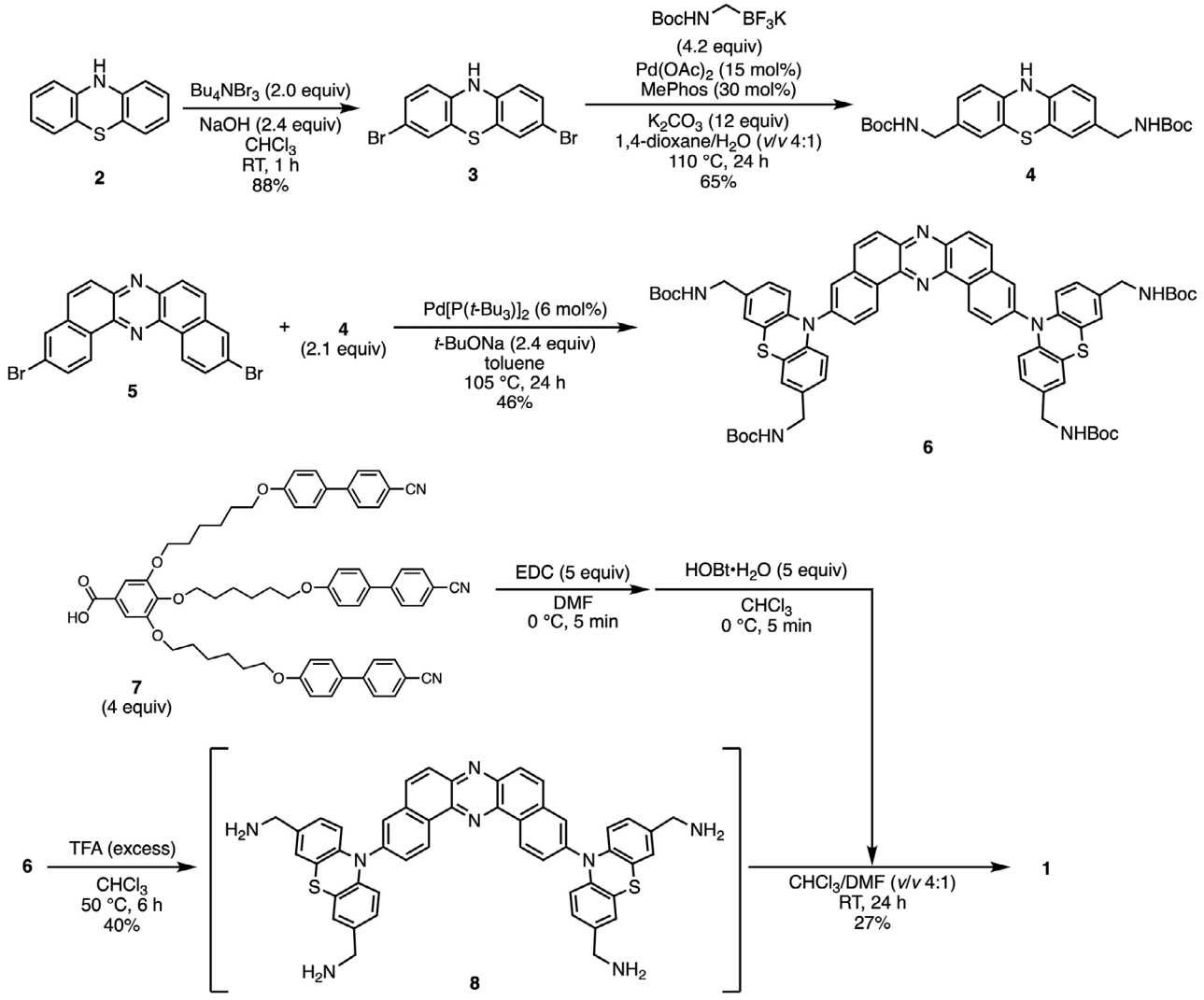

SCHEME 1 | Synthetic route to compound 1.

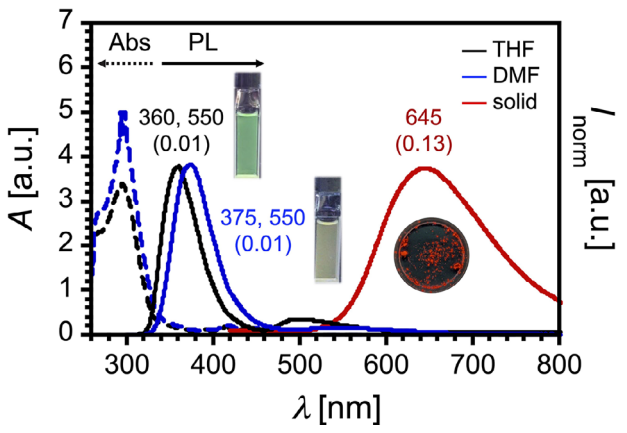

FIGURE 2 | UV-vis absorption and PL spectra of compound **1** in solutions ($c \sim 10^{-5}$ M) and in the solid state. Black dotted line: UV-vis absorption in THF; blue dotted line: UV-vis absorption in DMF; black solid line: PL in THF; blue solid line: PL in DMF; red solid line: PL in the solid state. Excitation wavelength: $\lambda_{ex} = 280$ nm. Values indicated on the PL spectra (and in parentheses) correspond to the emission maxima (nm) and absolute PLQY, determined using an integrated sphere.

mide **3** and *N*-Boc aminomethyltriflluoroborate [20] afforded bis(*N*-Boc aminomethyl)phenothiazine **4** in good yield. This electron-donating unit was subsequently coupled with 3,11-dibromodibenzophenazine **5** [23] to furnish the D–A–D-type intermediate **6**. Acidic deprotection of the *N*-Boc groups yielded intermediate **8**, which bears four aminomethyl substituents. Since the solubility of **8** in organic solvents is quite low, intermediate **8** was subsequently used for the final condensation protocol without isolation (see the Supporting Information for details). To incorporate self-assembling moieties into the fluorophore, the gallic acid derivative **7** [24] was activated with 1-ethyl-3-(3-dimethylaminopropyl)carbodiimide (EDC) and 1-hydroxybenzotriazole (HOBt), and subsequently condensed with **8** to afford the target compound **1**.

2.2 | Physicochemical and Phase-Transition Properties of 1

To elucidate the fundamental photophysical characteristics of compound **1**, dilute solutions were prepared in tetrahydrofuran (THF) and *N*,*N*-dimethylformamide (DMF). UV-vis absorption

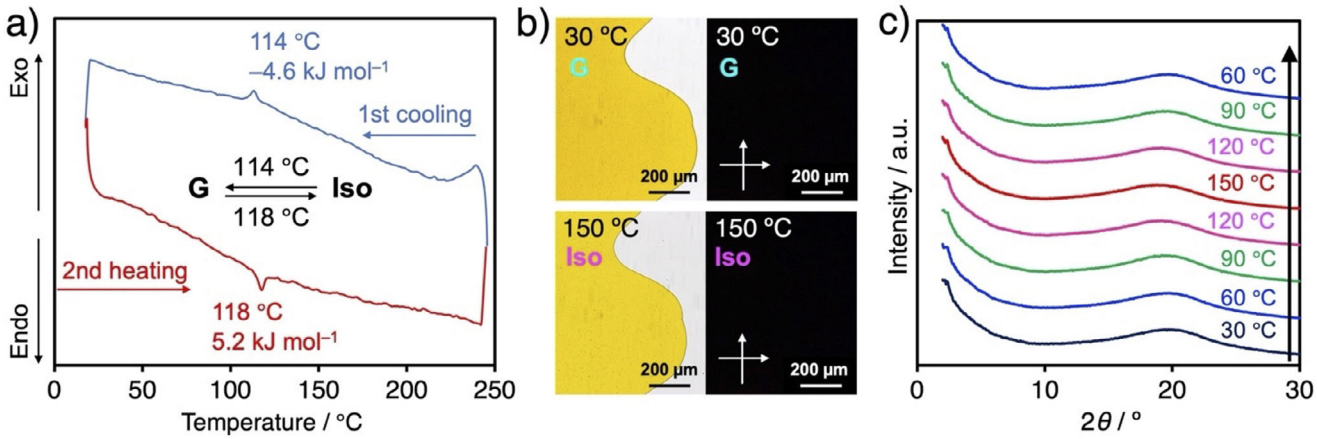

FIGURE 3 | (a) DSC thermogram of compound 1 at 10 °C min^{-1}. (b) Optical (left) and crossed polarized optical (right) images of compound **1** at 30 °C (top) and 150 °C (bottom). (c) PXRD patterns of compound **1** at different temperatures. Incident X-ray wavelength: $\lambda = 1.54$ Å. G and Iso represent glassy solid and isotropic liquid, respectively.

and photoluminescence (PL) spectra were subsequently recorded (Figure 2). The UV-vis absorption spectra of both solutions exhibited comparable profiles and absorption maxima, consistent with the photophysical properties of the D–A–D fluorophore we previously reported [18]. Notably, absorption bands attributed to charge-transfer (CT) transition were observed in the 450–500 nm range. Upon excitation with UV light (λ_{ex} = 280 nm), both solutions displayed weak dual emissions with peaks at 360–375 and 550 nm (Figure 2). This emission behavior contrasts with that of conventional D–A–D compounds, which typically exhibit dominant CT-type emission in polar solvents. The emission band around 360 nm is attributed to the monomer emission of cyanobiphenylene unit [25], which is reasonable given the presence of twelve such units in comparison to the single D–A–D core.

Interestingly, solidification of the solutions by evaporating solvents resulted in a pronounced red-shifted emission centered at λ_{em} = 645 nm, accompanied by an enhanced photoluminescence quantum yield (PLQY) of 0.13 (Figure 2). This aggregation-induced enhanced emission (AIEE) behavior is in stark contrast to that observed for previously reported D–A–D molecules [15, 18]. Accordingly, we further investigated the influence of molecular aggregation on the photophysical properties of compound **1**.

Since the compound **1** was expected to exhibit liquid-phase behavior, its phase-transition properties were investigated by differential scanning calorimetry (DSC), polarized optical microscopy (POM), and powder x-ray diffraction (PXRD). Upon heating on a hot stage, the initial powdered sample of compound **1** melted at approximately 130 °C, affording an orange-colored oily liquid. Upon cooling, the liquid solidified without a change in color, accompanied by a gradual decrease in fluidity. DSC analysis revealed a distinct endothermic peak at 118 °C on heating, with an associated enthalpy change of 5.2 kJ mol^{-1}. Upon cooling, an exothermic peak was observed at 114 °C, with a corresponding enthalpy change of 4.6 kJ mol^{-1} (Figure 3a). These results demonstrate a single, reversible phase transition in this temperature range. POM observations of compound **1** loaded into a glass cell showed no birefringence at temperatures either above or below the phase transition (Figure 3b), suggesting the absence of long-range periodic molecular orders. Furthermore, temperature-dependent PXRD patterns recorded from 30 °C to 150 °C exhibited only broad, featureless halos (Figure 3c). Taking all these data into account and contrary to our initial expectations, we concluded that compound **1** undergoes a single, reversible phase transition between a glassy solid and an isotropic liquid throughout the examined temperature range. Multiple intermolecular and intramolecular interactions involving π–π, hydrophobic, and hydrogen bonding ones may facilitate the non-periodic aggregation of compound **1**.

Figure 4a,b show the UV-vis and PL spectra of compound **1** in water/THF mixtures with varying water volume fraction (f_w) ranging from 0% to 90%, respectively. The UV-vis spectra exhibited stepwise changes depending on the f_w value (Figure 4a). In the f_w range of 0%–30%, the spectra remained largely unchanged. However, substantial spectral changes were observed between f_w = 40%–50%, where the absorption around 300 nm decreased, and a broad tail beyond 500 nm appeared, indicative of the onset of aggregation. From f_w = 60% to 90%, the spectra evolved further: the absorption around 300 nm partially recovered, while the long-wavelength tail above 500 nm persisted. These observations suggest that distinct aggregation states form depending on the f_w value.

The PL spectra showed even more pronounced changes (Figure 4b). In the f_w range of 0%–30%, the emission centered at λ_{em} = 360 nm gradually decreased in intensity. Starting from f_w = 40%, a new emission band around λ_{em} = 700 nm progressively emerged, coinciding with a reduction in the short-wavelength emission, resulting in dual-emission behavior (Figure 4b). Above f_w = 60%, the red-shifted emission became dominant as f_w increased. This gradual, ratiometric evolution in the PL profile as a function of f_w gives rise to a tunable emission color in the water/THF mixture, ranging from green to yellow, whitish orange, and ultimately bright orange (Figure 4c). The PLQY also increased with f_w above 60%, consistent with typical AIEE behavior.

Our previous work demonstrated that D–A–D fluorophores adopt flexible conformations and exists as a mixture of axial-axial (ax-

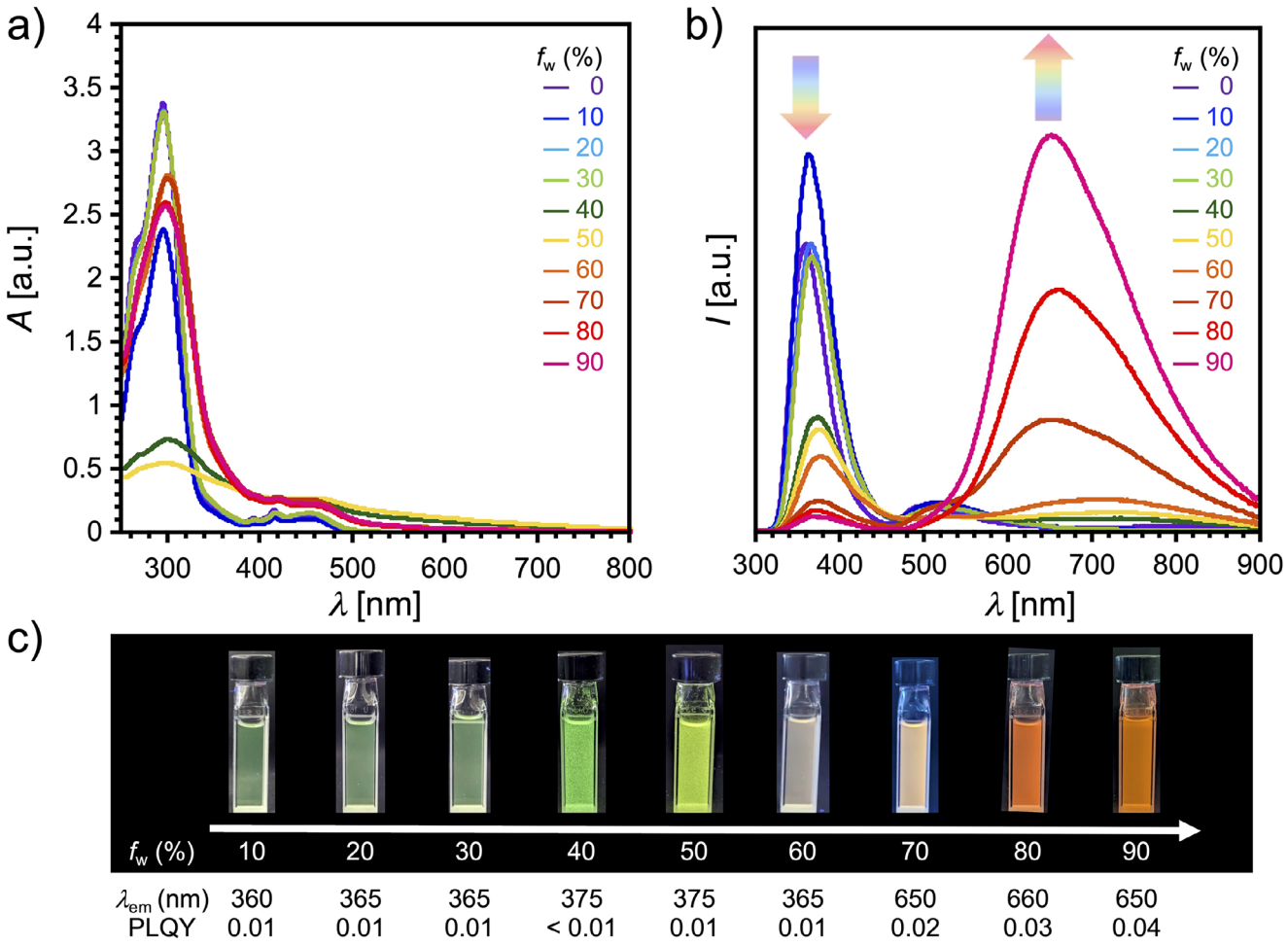

FIGURE 4 | (a) UV-vis absorption and (b) PL spectra of compound **1** in water/THF mixtures ($c \sim 10^{-5}$ M) with varying water volume fractions (f_w) from 0% to 90%. Excitation wavelength: $\lambda_{ex} = 280$ nm. (c) Photographs of compound **1** in water/THF mixtures under UV light irradiation ($\lambda_{ex} = 365$ nm).

ax), equatorial-equatorial (eq-eq), and axial-equatorial (ax-eq) conformers in the aggregated state in water [20]. In that case, dual emission was observed, arising from distinct conformers. In contrast, in the present study, only two emission bands were observed: one originating from the cyanobiphenylene moiety [22], and the other attributable to the eq-eq or eq-ax conformer of the D–A–D core. This observation implies the occurrence of ET from the high-energy emissive cyanobiphenylene units to the lower-energy D–A–D conformers, following the energy hierarchy of eq-eq < eq-ax < ax-ax [26].

Analysis of the UV-vis absorption spectrum of the aggregated state of compound **1**, in comparison with the PL spectrum of a cyanobiphenyl compound [22], revealed substantial spectral overlap, suggesting the possibility of Förster resonance energy transfer (FRET). Such aggregation-induced ET systems showing dual emission have been reported [27]. To further investigate this hypothesis, control experiments were performed by mixing a D–A–D compound **9** [18] and a cyanobiphenylene compound **10** (**9**:**10** = 1:4 molar ratio) in water/THF mixtures (Figure S1). As the f_w increased, the absorption spectrum of the **9**/**10** mixture shifted markedly in a manner similar to that of compound **1**, indicating that aggregation occurs at high f_w (Figure S1a). In contrast, the PL spectrum of the mixture exhibited a decrease in emission intensity at $\lambda_{em} = 370$ nm (attributed to compound **10**) as f_w increased up to 80% (Figure S1b). Moreover, no discernible emission appeared in the orange-to-red region (~650 nm), unlike the strong 650 nm emission observed for compound **1** (Figure S1b *vs.* Figure 4b). Nevertheless, at $f_w = 90\%$, the **9**/**10** mixture displayed a weak but broad emission centered at 650 nm (Figure S1b), implying that interrmolecular FRET can occur in the mixture and possibly within the aggregates of compound **1** as well.

To further elucidate the origin of aggregation-induced emissions in the 500–600 nm region, we performed f_w-dependent emission decay and excitation spectrum measurements for compound **1** (Figures S2 and S3, Tables S1 and S2). Time-correlated single photon counting (TCSPC) results revealed that the emission lifetime (τ) of the 370 nm component gradually increased as f_w rose from 0% to 60%, then decreased when f_w was further increased to 90% (Figure S2 and Table S1). In contrast, the τ of the 530 nm component increased monotonically with f_w (Figure S2b and Table S2). The excitation spectrum corresponding to the 370 nm emission in pure THF ($f_w = 0\%$) exhibited vibronic structure characteristic of the cyanobiphenylene unit. As f_w increased to 30%, this structure broadened and its intensity decreased with further water addition (Figure S3a), reflecting the strong aggregation tendency of the cyanobiphenylene units. In contrast, the excitation spectra for emissions at 530 and 650 nm

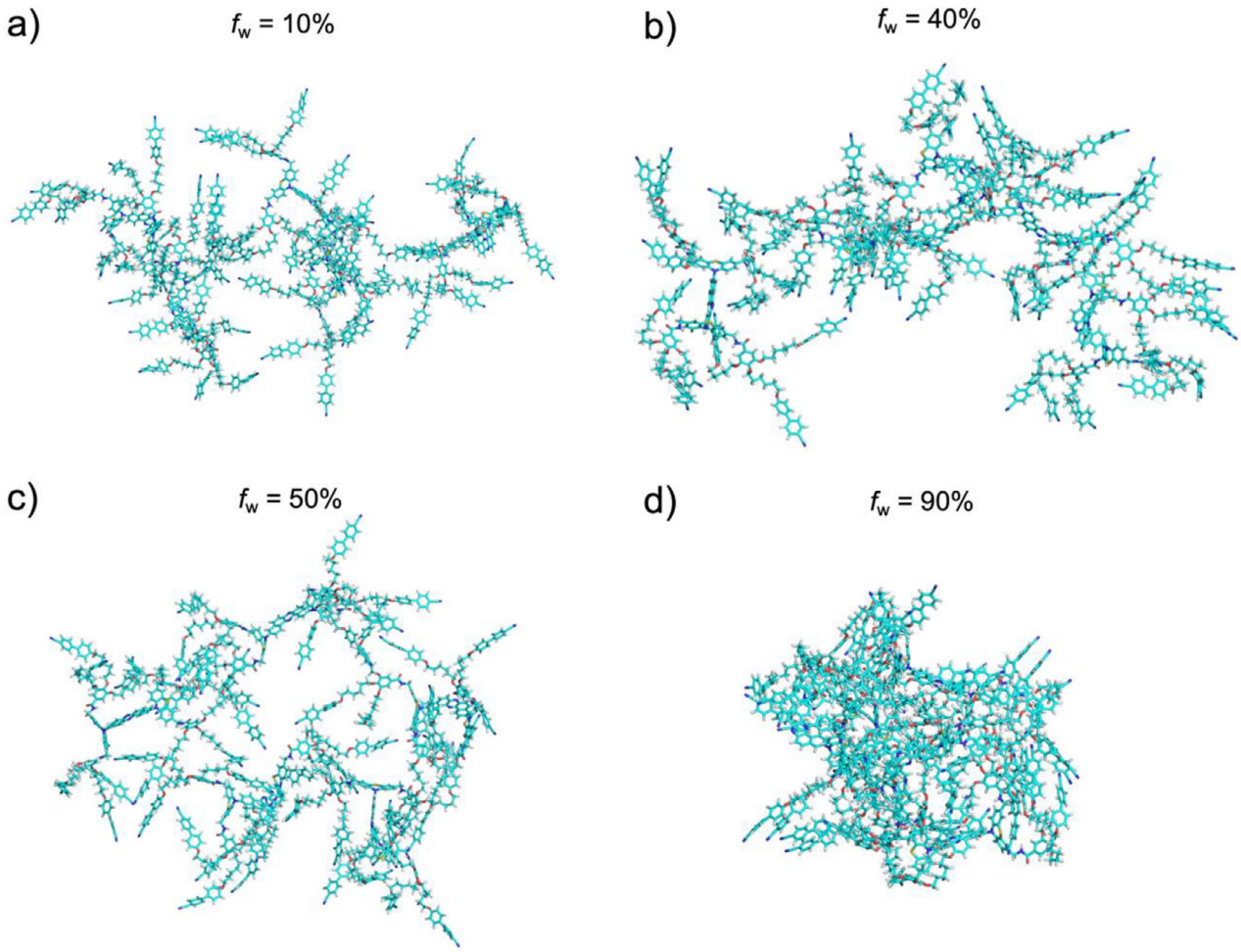

FIGURE 5 | Snapshots from MD simulation of compound **1** in the water/THF mixtures at 200 ns. The systems correspond to (a) $f_w = 10\%$, (b) $f_w = 40\%$, (c) $f_w = 50\%$, and (d) $f_w = 90\%$. Solvents molecules are omitted for clarity.

retained features characteristics of the D–A–D fluorophore core (Figure S3b,c), confirming that the newly emerging emissions in the 500–700 nm region originate from this core. The differences in emission wavelengths are consistent with previously reported conformation-dependent emissions [18]. Taken together, these findings indicate the presence of multiple emission pathways for compound **1** in water/THF mixtures depending on the aggregation state. At low f_w (0%–30%), cyanobiphenylene units begin to aggregate, leading to exciton delocalization along these units and a corresponding increase in τ for the 370 nm emission. At intermediate f_w (40%–70%), long-lived excitons on the cyanobiphenylene units can transfer energy to the D–A–D core through intra- and/or intermolecular FRET pathways.

2.3 | MD Simulation of Aggregation Formation of 1 in Water

To understand the microscopic aggregation behavior of D–A–D compound **1** in water/THF mixtures, we performed MD simulations at various water volume fractions (f_w = 10%, 40%, 50%, and 90%, Figure 5). In the initial structure for each simulation system, five molecules of compound were randomly distributed in the solvent.

The simulations revealed a strong dependence of the aggregation state on f_w. At a low water content (f_w = 10%), the molecules formed weak and transient aggregates characterized by intermittent dissociation and weak stacking of the cyanobiphenylene side chains (Figure 5a). At intermediate water fractions (f_w = 40% and 50%), stable but extended aggregates were formed, with infrequent π-stacking between the core or side-chain units (Figure 5b,c). In contrast, at high water content (f_w = 90%), the molecules coalesced into a single, dense, and spherical cluster (Figure 5d). A key structural feature of this cluster was that the central D–A–D units were shielded from direct contact with each other, being encapsulated by the cyanobiphenylene moieties. The compactness of the aggregates was quantified by the interatomic distance between the most distant atoms within the cluster at 200 ns, which was 6.43 nm for f_w = 90%, markedly smaller than for f_w = 40% (11.7 nm) and f_w = 50% (10.9 nm). These simulation results are in excellent agreement with experimental observations.

To identify the primary driving force for aggregation, we simulated two model compounds corresponding to the central D–A–D moiety (compound **9**) and the cyanobiphenylene side chain (compound 10) at f_w = 90% (Figure 6). The cyanobiphenylene molecules readily formed a spherical aggregate, mim-

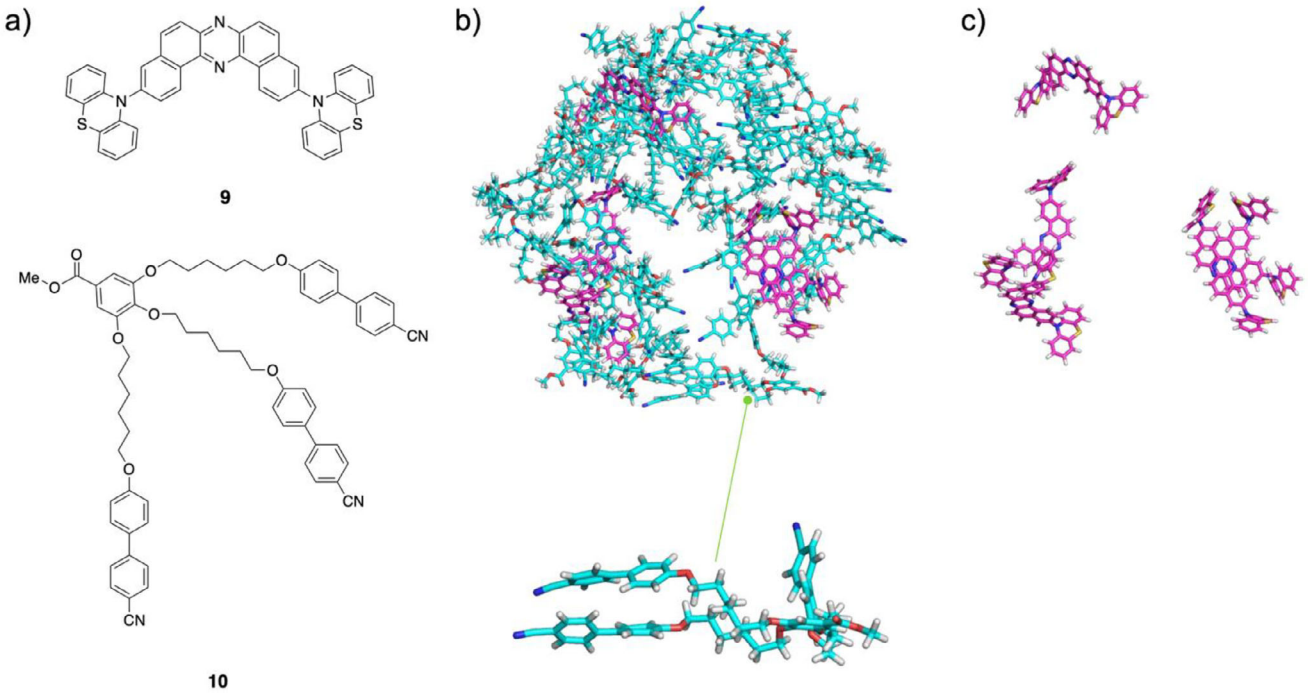

FIGURE 6 | (a) Chemical structures of compounds **9** and **10**. MD simulation snapshots at 200 ns: (b) aggregation formed by compounds **9** and **10** in a water/THF mixture (f_w = 90%) and (c) molecules of compound **9** extracted from the aggregation. Molecules of compounds **9** and **10** are shown in magenta and cyan, respectively. The enlarged view highlights a representative molecule of compound **10**.

icking the behavior of the parent compound **1**. Conversely, the π-core molecules remained largely dispersed. This clearly demonstrates that the hydrophobic interactions among the cyanobiphenylene moieties are the dominant force driving the self-assembly. This finding corroborates that, at f_w = 90%, the D-A-D units of compound **1** were surrounded by their cyanobiphenylene moieties, which would induce FRET from the cyanobiphenylene energy donor to the D–A–D energy acceptor.

3 | Conclusion

In summary, we have developed a new organic emitter based on a donor–acceptor–donor architecture incorporating multiple starburst-type hydrophobic mesogenic self-assembling units. Although the compound did not exhibit liquid crystalline behavior, it displayed a unique aggregation-induced ET phenomenon in aqueous environments. Molecular dynamics simulations supported the intramolecular organization of the hydrophobic units around the central fluorophore, facilitating efficient ET. This study opens a new avenue for the development of nano-ordered aggregate materials with tunable emission colors dependent on the degree of aggregation, potential for innovative sensing systems.

Acknowledgments

This work was supported by a Grant-in-Aid for Scientific Research (B) (JSPS KAKENHI Grant Number JP23K26730 and JP23K26545 for Youhei Takeda), a Grant-in-Aid for Scientific Research on Innovative Area "Aquatic Functional Materials: Creation of New Materials Science for Environment-Friendly and Active Functions (Area No. 6104)" (JSPS KAKENHI Grant Number JP19H05716 for Youhei Takeda, JP22H04540 for Tsuneaki Sakurai, and JP19H05718 for Go Watanabe), Japan Science and Technology Agency (JST) as part of Adopting Sustainable Partnerships for Innovative Research Ecosystem (ASPIRE) (Grant Number JPMJAP2425 for Youhei Takeda and Go Watanabe), and Research Grant (General Research) from TEPCO Memorial Foundation (for Youhei Takeda). Youhei Takeda and Satoshi Minakata acknowledge NIPPOH CHEMICALS for supplying *N*,*N*-diiodo-5,5-dimethylhydantoin (DIH). The computations were partially performed at the Research Center for Computational Science, Okazaki, Japan (Projects: 25-IMS-C039).

Conflicts of Interest

The authors declare no conflicts of interest.

Data Availability Statement

The data that supports the findings of this study are available in the supplementary material of this article

References

1. V. Coropceanu, J. Cornil, D. A. da Silva Filho, Y. Olivier, R. Silbey, J.-L. Brédas, "Charge Transport in Organic Semiconductors," *Chemical Reviews* 107 (2007): 926–952, https://doi.org/10.1021/cr050140x.

2. C. Wang, H. Dong, W. Hu, Y. Liu, D. Zhu, "Semiconducting π-Conjugated Systems in Field-Effect Transistors: A Material Odyssey of Organic Electronics," *Chemical Reviews* 112 (2012): 2208–2267, https://doi.org/10.1021/cr100380z.

3. J. Gierschner, J. Cornil, H.-J. Egelhaaf, "Optical Bandgaps of π-Conjugated Organic Materials at the Polymer Limit: Experiment and Theory," *Advanced Materials* 19 (2007): 173–191, https://doi.org/10.1002/adma.200600277.

4. A. Khasbaatar, Z. Xu, J.-H. Lee, "From Solution to Thin Film: Molecular Assembly of π-Conjugated Systems and Impact on (Opto)Electronic Properties," *Chemical Reviews* 123 (2023): 8395–8487, https://doi.org/10.1021/acs.chemrev.2c00905.

5. A. J. C. Kuehne, M. C. Gather, "Organic Lasers: Recent Developments on Materials, Device Geometries, and Fabrication Techniques," *Chemical Reviews* 116 (2016): 12823–12864, https://doi.org/10.1021/acs.chemrev.6b00172.

6. O. Ostroverkhova, "Organic Optoelectronic Materials: Mechanisms and Applications," *Chemical Reviews* 116 (2016): 13279–13412, https://doi.org/10.1021/acs.chemrev.6b00127.

7. M. Dai, Y. J. Yang, S. Sarkar, K. H. Ahn, "Strategies to Convert Organic Fluorophores Into Red/Near-Infrared Emitting Analogues and Their Utilization in Bioimaging Probes," *Chemical Society Reviews* 52 (2023): 6344–6358, https://doi.org/10.1039/D3CS00475A.

8. Z. Li, J. R. Askim, K. S. Suslick, "The Optoelectronic Nose: Colorimetric and Fluorometric Sensor Arrays," *Chemical Reviews* 119 (2019): 231–292, https://doi.org/10.1021/acs.chemrev.8b00226.

9. X. Wu, S. Ni, C.-H. Wang, W. Zhu, P.-T. Chou, "Comprehensive Review on the Structural Diversity and Versatility of Multi-Resonance Fluorescence Emitters: Advance, Challenges, and Prospects Toward OLEDs," *Chemical Reviews* 125 (2025): 6685–6752, https://doi.org/10.1021/acs.chemrev.5c00021.

10. J. Luo, Z. Xie, J. W. Y. Lam, "Aggregation-Induced Emission of 1-methyl-1,2,3,4,5-pentaphenylsilole," *Chemical Communications* (2001): 1740–1741, https://doi.org/10.1039/b105159h.

11. Y. Hong, J. W. Y. Lam, B. Z. Tang, "Aggregation-Induced Emission: Phenomenon, Mechanism and Applications," *Chemical Communications* (2009): 4332–4353, https://doi.org/10.1039/b904665h.

12. J. Mei, N. L. Leung, R. T. K. Kwok, J. W. Y. Lam, B. Z. Tang, "Aggregation-Induced Emission: Together We Shine, United We Soar!," *Chemical Reviews* 115 (2015): 11718–11940, https://doi.org/10.1021/acs.chemrev.5b00263.

13. T. Wu, J. Huang, Y. Yan, "Self-Assembly of Aggregation-Induced-Emission Molecules," *Chemistry—An Asian Journal* 14 (2019): 730–750, https://doi.org/10.1002/asia.201801884.

14. Y. Takeda, "Modulating the Photophysical Properties of Twisted Donor–Acceptor–Donor π-Conjugated Molecules: Effect of Heteroatoms, Molecular Conformation, and Molecular Topology," *Accounts of Chemical Research* 57 (2024): 2219–2232, https://doi.org/10.1021/acs.accounts.4c00353.

15. P. Data, P. Pander, M. Okazaki, Y. Takeda, S. Minakata, A. P. Monkman, "Dibenzo[*a*,*j*]phenazine-Cored Donor–Acceptor–Donor Compounds as Green-to-Red/NIR Thermally Activated Delayed Fluorescence Organic Light Emitters," *Angewandte Chemie International Edition* 55 (2016): 5739–5744, https://doi.org/10.1002/anie.201600113.

16. S. Izumi, H. F. Higginbotham, A. Nyga, "Thermally Activated Delayed Fluorescent Donor–Acceptor–Donor–Acceptor π-Conjugated Macrocycle for Organic Light-Emitting Diodes," *Journal of the American Chemical Society* 142 (2020): 1482–1491, https://doi.org/10.1021/jacs.9b11578.

17. H. F. Higginbotham, M. Okazaki, P. de Silva, S. Minakata, Y. Takeda, P. Data, "Heavy-Atom-Free Room-Temperature Phosphorescent Organic Light-Emitting Diodes Enabled by Excited States Engineering," *ACS Applied Materials & Interfaces* 13 (2021): 2899–2907, https://doi.org/10.1021/acsami.0c17295.

18. M. Okazaki, Y. Takeda, P. Data, "Thermally Activated Delayed Fluorescent Phenothiazine–dibenzo[*a*,*j*]phenazine–phenothiazine Triads Exhibiting Tricolor-Changing Mechanochromic Luminescence," *Chemical Science* 8 (2017): 2677–2686, https://doi.org/10.1039/C6SC04863C.

19. Y. Takeda, H. Mizuno, Y. Okada, "Hydrostatic Pressure-Controlled Ratiometric Luminescence Responses of a Dibenzo[*a*,*j*]phenazine-Cored Mechanoluminophore," *ChemPhotoChem* 3 (2019): 1203–1211, https://doi.org/10.1002/cptc.201900190.

20. T. Enjou, S. Goto, Q. Liu, "Water-Dispersible Donor–Acceptor–Donor π-conjugated Bolaamphiphiles Enabling a Humidity-Responsive Luminescence Color Change," *Chemical Communications* 60 (2024): 3653–3656, https://doi.org/10.1039/D3CC05749F.

21. G. W. Gray, K. J. Harrison, J. A. Nash, "New Family of Nematic Liquid Crystals for Displays," *Electronics Letters* 9 (1973): 130–131, https://doi.org/10.1049/el:19730096.

22. D. Chen, F. Tenopala-Carmona, J. A. Knöller, "Mesogenic Groups Control the Emitter Orientation in Multi-Resonance TADF Emitter Films**," *Angewandte Chemie International Edition* 62 (2023): e202218911, https://doi.org/10.1002/anie.202218911.

23. Y. Takeda, M. Okazaki, S. Minakata, "Oxidative Skeletal Rearrangement of 1,1′-binaphthalene-2,2′-diamines (BINAMs) via C–C Bond Cleavage and Nitrogen Migration: A Versatile Synthesis of U-Shaped Azaacenes," *Chemical Communications* 50 (2014): 10291–10294, https://doi.org/10.1039/C4CC04911J.

24. A. Gandubert, M. Amela-Cortes, S. K. Nayak, "Tailoring the Self-Assembling Abilities of Functional Hybrid Nanomaterials: From Rod-Like to Disk-Like Clustomesogens Based on a Luminescent $\{Mo_6Br_8\}^{4+}$ Inorganic Cluster Core," *Journal of Materials Chemistry C* 6 (2018): 2556–2564, https://doi.org/10.1039/C7TC05412B.

25. T. Ikeda, S. Kurihara, S. Tazuke, "Excimer Formation Kinetics in Liquid-Crystalline Alkylcyanobiphenyls," *Journal of Physical Chemistry* 94 (1990): 6550–6555, https://doi.org/10.1021/j100380a008.

26. P. Data, M. Okazaki, S. Minakata, Y. Takeda, "Thermally Activated Delayed Fluorescence vs. Room Temperature Phosphorescence by Conformation Control of Organic Single Molecules," *Journal of Materials Chemistry C* 7 (2019): 6616–6621, https://doi.org/10.1039/C9TC00909D.

27. M. Deniβen, R. Hannen, D. Itskalov, "One-Pot Synthesis of a White-Light Emissive Bichromophore Operated by Aggregation-Induced Dual Emission (AIDE) and Partial Energy Transfer," *Chemical Communications* 56 (2020): 7407–7410.

Supporting Information

Additional supporting information can be found online in the Supporting Information section.

Supporting Information file 1: asia70426-sup-0001-SuppMat.pdf